Published in final edited form as:
J Cereb Blood Flow Metab. 2008 November ; 28(11): 1771–1785. doi:10.1038/jcbfm.2008.76.

Transcriptomic screening of microvascular endothelial cells implicates novel molecular regulators of vascular dysfunction after spinal cord injury

Richard L Benton[1,2,3], **Melissa A Maddie**[1,2], **Christopher A Worth**[4], **Edward T Mahoney**[1,2], **Theo Hagg**[1,2,5], and **Scott R Whittemore**[1,2,3]

[1]Kentucky Spinal Cord Injury Research Center, University of Louisville School of Medicine, Louisville, Kentucky, USA

[2]Department of Neurological Surgery, University of Louisville School of Medicine, Louisville, Kentucky, USA

[3]Department of Anatomical Sciences and Neurobiology, University of Louisville School of Medicine, Louisville, Kentucky, USA

[4]Brown Cancer Center, University of Louisville School of Medicine, Louisville, Kentucky, USA

[5]Department of Pharmacology and Toxicology, University of Louisville School of Medicine, Louisville, Kentucky, USA

Abstract

Microvascular dysfunction is a critical pathology that underlies the evolution of secondary injury mechanisms after traumatic spinal cord injury (SCI). However, little is known of the molecular regulation of endothelial cell (EC) plasticity observed acutely after injury. One reason for this is the relative lack of methods to quickly and efficiently obtain highly enriched spinal microvascular ECs for high-throughput molecular and biochemical analyses. Adult C57Bl/6 mice received an intravenous injection of fluorescein isothiocyanate (FITC)-conjugated *Lycopersicon esculentum* lectin, and FITC-lectin-bound spinal microvessels were greatly enriched by fluorescence-activated cell sorter (FACS) purification. This technique allows for rapid (< 1.5 h postmortem) isolation of spinal cord microvascular ECs (smvECs). The results from cell counting, reverse-transcription polymerase chain reaction (RT-PCR), and western blot analyses show a high degree of EC enrichment at mRNA and protein levels. Furthermore, a focused EC biology microarray analysis identified multiple mRNAs dramatically increased in the EC compartment 24 h after SCI, which is a time point associated with the pathologic loss of spinal vasculature. These included thrombospondin-1, CCL5/RANTES, and urokinase plasminogen activator, suggesting they may represent targets for therapeutic intervention. Furthermore, these novel methodologic approaches will likely facilitate the discovery of molecular regulators of endothelial dysfunction in a variety of central nervous system (CNS) disorders including stroke and other neurodegenerative diseases having a vascular component.

Correspondence: Dr RL Benton, University of Louisville School of Medicine, Kentucky Spinal Cord Research Center, 511 South Floyd Street, MDR 616, Louisville, KY 40292, USA. rlbent01@louisville.edu.

Disclosure The contents of this study are solely the responsibility of the authors and do not necessarily represent the official views of the NIH.

Keywords

flow cytometry; PAI-1; spinal cord injury; TSP-1; uPA

Introduction

Traumatic spinal cord injury (SCI) is a devastating disorder for which there is currently no single effective treatment. Interestingly, the most promising results have been obtained using agents that exhibit potent vasoactive properties (Geisler *et al*, 2001; Grasso *et al*, 2006; Pannu *et al*, 2007). These results suggest that future therapies targeting specific pathways/events associated with vascular dysfunction after SCI may hold great promise. Thus, a better understanding of the precise molecular control of vascular pathology in the injured central nervous system (CNS) is critical for the rational development of successful vasoactive therapeutics.

Physical trauma to the spinal cord results in immediate damage to the delicate vasculature and the loss of perfusion, especially within the highly vascularized gray matter. The shearing of micro-vessels at the injury epicenter results in hemorrhage, the degree of which correlates with both terminal histopathology and functional deficit (Noble and Wrathall, 1989). This hemorrhage results in additional immediate damage by the vasogenic edema formation (Yang *et al*, 1994), excitotoxicity (Bullock and Fujisawa, 1992), infiltration of circulating leukocytes (Means and Anderson, 1983), as well as further loss of blood flow because of vasoconstriction in the spared epicenter and penumbral blood vessels (Ducker and Assenmacher, 1969). This vascular dysfunction continues at the injury site for days to weeks after SCI, with the loss of vascular support initiating an endogenous angiogenic response, leading to neovascularization of the affected tissue (Loy *et al*, 2002; Casella *et al*, 2002). However, these newly formed blood vessels never acquire mature phenotypes, showing hyperpermeability and immature tight junctional phenotypes (Whetstone *et al*, 2003; Benton *et al*, 2008). The cellular and molecular events contributing to this second phase of vascular dysfunction after SCI remain poorly understood, partially because of the lack of methods to isolate pure populations of endothelial cells (ECs) from the injured spinal cord suitable for high-throughput molecular analyses.

Although several protocols exist for the isolation of CNS microvascular ECs from the brain (Diglio *et al*, 1982; Hemmings and Storey, 1999; Wu *et al*, 2003), only two reports exist describing the primary isolation of microvessels from the porcine (Joo *et al*, 1982) and murine (Ge and Pachter, 2006) spinal cord. A major issue related to these approaches relates to the purity of the resultant microvascular EC preparation as well as to the time associated with obtaining the cells, both issues making them unsuitable for polymerase chain reaction (PCR)-based molecular analyses of the mRNA content (Yousif *et al*, 2007).

In this study, we describe a novel methodology for the rapid isolation of highly enriched spinal ECs from the intact and injured mouse spinal cord, using a combination of intravital lectin administration to label spinal microvessels followed by fluorescence-activated cell sorter (FACS) purification. Furthermore, these preparations are well suited for high-through-put analyses of mRNA expression. We show that several mRNAs and proteins are highly dysregulated immediate time points associated with overt loss of vascular support after SCI in the endothelial compartment. The results from this study implicate several molecules, which are well-established effectors of EC/neurovascular unit (NVU) plasticity, but are novel in the context of SCI. Furthermore, future studies using the methodologies reported here may result in the elucidation of other pathologic cascades potentiated within the EC compartment and lead to new therapeutic possibilities in other CNS pathologies with vascular components.

Materials and methods

Spinal Cord Injuries

All surgical intervention and subsequent care and treatment of all animals used in this study were in strict accordance with the PHS Policy on Humane Care and Use of Laboratory Animals and University of Louisville IACUC guidelines. A total of 48 adult female C57Bl/6 mice (18 to 20 g, Harlan, Indianapolis, IN, USA) were anesthetized using a 1.2% avertin solution (2,2,2-tribromoethanol) administered at 240 mg/kg intraperitoneally and prepared as previously described (Benton *et al*, 2008). Once anesthesia was achieved, the surgical site was prepared by shaving and by a Betadine scrub, and laminectomies were performed at the T7/8 vertebral level, exposing the T9/10 spinal cord segment. Without opening the dura, mice received a moderate contusive SCI (50 kdyn force per 500 to 600 μm displacement) using the IH impactor (Infinite Horizons Inc., Lexington, KY, USA). The incision sites were then closed in layers and a topical antibiotic (Bacitracin) was applied to the incision site. Animals received prophylactic injections of gentamicin to prevent infection (1 mg/kg, intramuscularly), and a 2 ml bolus subcutaneous injection of saline was administered to prevent perioperative dehydration. Mice were housed five per cage and cages were placed on a 37°C heating pad overnight. In addition, immediately after surgery and for 72 h postoperatively, animals also received twice daily injections of buprenorphine (Buprenex; 0.075 mg/kg, subcutaneouly) and their bladders were manually expressed twice daily.

Intravascular Lectin Administration

Spinal microvessels in control and injured mouse spinal cords were intravascularly labeled using 100 μg of fluorescein isothiocyanate (FITC)-conjugated *Lycopersicon esculentum* agglutinin (LEA) lectin (FL-1171, 2 mg/ml; Vector Laboratories Inc., Burlingame, CA, USA). At 0 or 3 days after SCI, mice were deeply anesthetized as described above, and FITC-LEA was delivered systemically by an intravenous injection into the surgically exposed right external jugular vein. A volume of 50 μl of FITC-LEA was administered to each mouse at a rate of 1.2 mL/h using a syringe pump (model no. 780100, KD Scientific, Holliston, MA, USA). Fluorescein isothiocyanate-conjugated *Lycopersicon esculentum* agglutinin lectin was allowed to circulate for 15 mins before perfusion with saline. For isolation of microvascular ECs, 3 mm of spinal cord including the injury epicenter was rapidly isolated and processed as described below. For immunohistochemical processing, spinal tissue spanning the injury epicenter with 5 mm of adjacent rostral and caudal spinal segments was dissected and processed as described below.

Immunohistochemistry

Spinal cords were dissected from spinal columns, placed in mounting medium (Triangle Biomedical Sciences, Durham, NC, USA), and sectioned at 20 μm on a cryostat, and slides were stored at −80°C until use. On the day of staining, spinal cord tissue was then postfixed in ice-cold methanol for 10 mins. Tissue was then blocked in 0.1 M tris-buffered saline (TBS), 0.1% Triton X-100, 0.5% bovine serum albumin, and 10% normal donkey serum for 1 h at room temperature. Astrocytes were identified using a rabbit polyclonal anti-GFAP antibody (Z0334, 1:500 dilution; immunogen: glial fibrillary acidic protein (GFAP) isolated from cow spinal cord; Dako, Carpinteria, CA, USA). Neurons were identified using a rabbit polyclonal anti-Map2 antibody (AB5622, 1:200 dilution; immunogen: microtubule-associated protein purified from the rat brain; Chemicon, Temecula, CA, USA). Oligodendrocytes were visualized using a rabbit polyclonal anti-OSP/claudin-11 antibody (36-4500, 1:150 dilution; immunogen: synthetic peptide derived from the C-terminal region of human OSP/claudin-11, which differs by only one amino acid from mouse and rat sequences; Zymed Laboratories, Carlsbad, CA, USA). Vascular ECs were identified using a monoclonal rat anti-PECAM-1 antibody (550274, clone MEC13.3, 1:50 dilution; immunogen: cell membrane fractions from

mouse-derived EC line tEnd.1; BD Pharmingen, San Diego, CA, USA), or a polyclonal rabbit anti-von Willebrand factor/factor VIII antibody (A0082, 1:200 dilution; immunogen: von Willebrand factor/factor VIII purified from human plasma; Dako), or a polyclonal rabbit anti-glucose transporter type I (Glut-1) antibody (AB1340, 1:100 dilution; immunogen: a synthetic peptide corresponding to the internal domain of the C terminus of rat Glut-1; Chemicon), or a polyclonal rabbit anti-claudin V (clone Z43.JK, 1:50; immunogen: synthetic peptide derived from C-terminal sequence of mouse claudin 5; Zymed Laboratories). The specificity of staining for each antibody was shown by replacing the antibody with preimmune serum obtained from the appropriate species, which resulted in no staining. The sections were then incubated with rhodamine-conjugated (TRITC; 1:200) secondary antibodies (Jackson ImmunoResearch Laboratories Inc., West Grove, PA, USA) for 1 h at room temperature in a humidified chamber. All photomicro-graphs showing immunostained spinal cord sections were captured using either a Nikon TE 300 inverted microscope equipped with a Spot CCD camera and capture software (Diagnostic Instruments Inc., Sterling Heights, MI, USA) or an Eclipse C1 laser confocal microscope (Nikon Instruments Inc., Melville, NY, USA).

Isolation of Spinal Cord Microvascular Endothelial Cells

For isolation of spinal cord microvascular endothelial cells (smvECs), spinal tissue was rapidly dissected from spinal columns, with 3 mm taken spanning SCI epicenters for 24 h SCI samples. Tissue was then homogenized in Hank's balanced salt solution on ice for 3 mins using an electric homogenizer (Model TH01; Omni International, Marietta, GA, USA) set at midspeed. The crude homogenate was then triturated using three passes through a 26-gauge needle followed by three passes through a 30-gauge needle. The sample was then sieved using a 70 μm mesh tube insert (BD Falcon, Bedford, MA, USA). Samples were then subjected to FACS using a MoFlo system (DAKO, Ft Collins, CO, USA). The samples were loaded and once cell flow was established, the triggering setting was reconfigured from cell size to fluorescence. Event triggering is based on the fluorescence of the FITC-LEA-bound microvascular fragments at an excitation of 488 nm and detection at 530/40 nm. The brightest population of cells was selected with the sort region, with previous experiments verifying that only this population contained the target fragments (see Figure 3).

Western Blotting

Tissue and pelleted FACS-sorted microvascular fragments were sonicated in lysis buffer consisting of 100 mmol/L Tris (pH 7.4), 1% SDS (sodium dodecyl sulfate), and 1 × protease inhibitor cocktail (Mini-complete, EDTA (ethylenediaminetetraacetic acid) free, Boehringer Mannheim Inc., GmbH, Mannheim, Germany). Protein concentrations were estimated by bicinchoninic acid (BCA) assay (Pierce Biotechnology Inc., Rockford, IL, USA). Equal amounts of proteins were separated on a Tris-glycine 4% to 12% gradient precast gel (Invitrogen, San Diego, CA, USA), transferred to a nitrocellulose membrane, and immuno-blotted using the rabbit polyclonal antibodies listed in the immunohistochemical methods description at 1:1,000 (claudin-5), 1:2,000 (GFAP, occludin), or 1:10,000 (NSE (neuron-specific enolase), CNPase) dilutions. For semi-quantitative densitometric analyses of western blotting results, blots were terminally probed using a rabbit anti-β-actin (1:10,000; Novus Biologicals, Littleton, CO, USA) to serve as a normalizing immunosignal. All secondary antibodies used for immunoblotting were biotinylated goat anti-rabbit antibodies (Vector Laboratories Inc.). Proteins were detected using enhanced chemiluminescence (ECL Plus; Amersham, Piscataway, NJ, USA). Equal loading and uniform transfer of proteins in different lanes were verified by staining the transferred nitrocellulose membrane with Ponceau S stain. Immunoblots were quantified by densitometric analysis using Imagequant software (Molecular Devices Inc., Sunnyvale, CA, USA).

Urokinase Plasminogen Activator and Plasmin Zymography

For plasmin zymography, soluble protein isolated from spinal cord tissue was loaded on precast Novex 4% to 16% Zymogram Blue Casein Gels. The gels were then run under nondenaturing conditions in Tris-glycine SDS running buffer. For standardization, 0.5 and 1.0 μg of plasmin from human plasma (Sigma, St Louis, MO, USA) were loaded onto each gel. After electrophoresis, gels were washed in Zymogram renaturing buffer, followed by zymogram developing buffer overnight at 37°C. All reagents for plasmin zymography were obtained from Invitrogen. For the detection of uPA enzymatic activity, proteins from affected spinal cord tissues were resolved under nonreducing conditions on 10% SDS-polyacrylamide gels containing 0.01 U/mL plasminogen and 1.5 mg/mL gelatin (Sigma). For standardization, 10 pg of rat uPA (American Diagnostica Inc., Stamford, CT, USA) was loaded onto each gel. After electrophoresis, the gels were washed three times in 2.5% Triton X-100 solution and then incubated in 100 mmol/L Tris-HCl (pH 8.2) buffer for 18 h at 371C. The gels were then stained with 0.1% Amido black solution. Zymograms were quantified by densitometric analysis using Imagequant software (Molecular Devices Inc.).

Reverse-Transcription Polymerase Chain Reaction Analysis of Endothelial Cell Gene Expression

For RNA isolation from mouse spinal tissue, spinal cords were sonicated in TRIZOL® Reagent (Invitrogen Inc., Carlsbad, CA) and extracted following the manufacturer's protocol. For RNA isolation from FACS-sorted smvECs, the PicoPuret™ RNA Isolation Kit (Arcturus Bioscience Inc., Mountain View, CA, USA) was used according to the manufacturer's protocol. After RNA isolation, 1 μg of total RNA from the total spinal cord and FACS-isolated smvECs was reverse-transcribed into cDNA in reactions containing Moloney-Murine Leukemia Virus Reverse Transcriptase (M-MLV RT) (100 U, Promega, Madison, WI, USA), DTT (dithiothreitol; 5 mmol/L), dNTPs (deoxyribonucleotide triphosphate; 1 mmol/L each), random hexamers (4 μg), and RNAse inhibitor (20 U, Boehringer Mannheim Inc.). Polymerase chain reaction was performed using specific primers obtained from Invitrogen Inc. for cyclophilin A (forward: 5′-CGGAGAGAAATTTGAGGATGAGA-3′; reverse: 5′-AGTCTTGGCAGTGCAGATAAAA-3′), Map2 (forward: 5′-GACGAGCGGAAAGATGAA-3′; reverse: 5′-TGGAAATCCATTGGCG-3′), OSP/claudin-11 (forward: 5′-ATGGTAGCCACTTGCCTT-3′; reverse: 5′-TTTGCAGTGGTAGAGACCAG-3′), GFAP (forward: 5′-TCCTGGAACAGCAAAACAAG-3′; reverse: 5′-CAGCCTCAGGTTGGTTTCAT-3′), Desmin (forward: 5′-GGCTCCTCGAGTTCAATGACAT-3′; reverse: 5′-TAGTTGGCGAAGCGGTCATT-3′), platelet/endothelial cell adhesion molecule-1 (PECAM-1) (forward: 5′-TGCTCTATGCAAGCCT-3′; reverse: 5′-CTTCACCTCGTACTCAATC-3′), Glut-1 (forward: 5′-GCTGTGCTTATGGGCTTCTC-3′; reverse: 5′-CACATACATGGGCACAAAGC-3′), and claudin-5 (forward: 5′-GCTCTCAGAGTCCGTTGACC-3′; reverse: 5′-CTGCCCTTTCAGGTTAGCAG-3′). Optimum annealing temperatures, cycle numbers, and reverse transcription (RT) input were empirically determined by amplification of a single PCR product at the appropriate molecular weight for each target cDNA. All RT and PCR reactions were performed using a PTC-200 gradient thermocycler (MJ Research, Reno, NV, USA) using 25 cycles of amplification except for desmin where 35 cycles of amplification was performed. Polymerase chain reaction products were analyzed by native polyacrylamide gel electrophoresis followed by resolution by SYBR gold staining (Molecular Probes, Eugene OR, USA). Relative quantitation was carried out by densitometric analysis of amplicon production using ImageQuant software (v. 5.1; GE Healthcare, Piscataway, NJ, USA).

Focused Microarray Analysis

After FACS isolation, smvECs obtained from control and injured spinal cord tissue were pelleted by centrifugation at 14,000 r.p.m. at 4°C for 15 mins. Total RNA was isolated using the PicoPure RNA Isolation Kit (Arcturus Bioscience Inc.) according to the manufacturer's protocol. Total RNA was reverse transcribed using the ReactionReadyt™ First Strand cDNA Synthesis Kit (SuperArray Bioscience Corp., Frederick, MD, USA) according to the recommended protocol. Differential EC gene expression was then ascertained using the RT^2Profilert™ PCR Array (Cat. no. APMM-015; mouse, endothelial cell biology PCR array; SuperArray Bioscience Corp.). All real-time polymerase chain reaction (qRT-PCR) reactions were performed using an ABI 7900 real-time PCR instrument, and results analyzed using the EXCEL analysis template was provided by SuperArray Bioscience Corp.

Statistical Analyses

All quantitative data are expressed as mean±s.d. Differences between the two groups (FACS results, immunoblot data, and SCI microarray results) were compared using Student's *t*-test. One-way analysis of variance followed by Tukey's HSD post *hoc* analysis was used to compare results for plasmin and uPA enzymatic activity. Statistical significance was defined at $P \leq 0.05$.

Results

Intravascular Fluorescein Isothiocyanate-conjugated *Lycopersicon esculentum* Agglutinin Specifically Binds Perfused Spinal Cord Vessels

Previous studies have shown that various lectins, including LEA, bind specifically to the luminal glycocalyx of perfused vessels in various tissue types including spinal microvessels (Lin *et al*, 2007). Consistent with these results, we observed specific interaction with perfused endothelium in the mouse spinal cord after intravascular administration of FITC-LEA (Figure 1). Perfused microvessels were apparent in both spinal white and gray matters, with the relative hypervascularity of spinal gray matter clearly showed using this intravital technique (Figure 1A). This interaction of the FITC-LEA and the endothelial glycocalyx is specific and not the result of the perivascular entrapment of tracer as shown by a lack of spinal microvascular staining when a comparable dose (100 μg) of molecular weight-matched dextran (100 to 110 kDa average size) was delivered intravascularly (Figure 1B). In spinal gray matter, FITC-LEA binding was not associated with neurons (Map2; Figure 1C), astrocytes (GFAP; Figure 1D), or oligodendrocytes (OSP; Figure 1E). In contrast, FITC-LEA binding was clearly associated with smvECs as shown by colocalization with immunostaining for the well-established EC markers PECAM-1, Glut-1, and claudin-5 (Figures 1F to 1H).

Fluorescence-Activated Cell Sorter Isolation of Fluorescein Isothiocyanate-Conjugated *Lycopersicon esculentum* Agglutinin-Bound Spinal Cord Microvascular Endothelial Cells Yields a Highly Enriched Cellular Preparation

To assess the pre- and postsort enrichment of ECs, small aliquots of sample (5 μl) were added to Hoechst dye, placed on a microscope slide, cover-slipped, and mounted for analysis. In the presort samples, FITC-bound spinal microvessels and their associated nuclei are apparent (arrows, Figure 2A), although they represent a minority of the total cellular population. After FACS enrichment, many FITC-bound microvascular fragments are observed, with very few nonvascular nuclei observed (arrowheads, Figure 2B). Quantitative data (Figure 2F) show that in crude spinal cord homogenate, the vascular EC content represents approximately 10% of all cells present per unit volume. After FACS, the EC fraction is significantly increased to approximately 90% of the total cell population. This estimation of purity is likely conservative because it is feasible that some nonvascular-associated nuclei are possibly ECs that have become dislodged from the spinal microvascular fragments because of shear flow stress as the

cells pass through the instrument. Consistent with this interpretation is the significant decrease in the morphologic complexity of the microvascular fragments after FACS purification (Figure 2E). Fluorescence-activated cell sorter-enriched samples were obtained by collecting the brightest population of cells (R1 gate, Figure 2D), which exhibited FITC intensity an order of magnitude higher than the background cellular population. Few FITC-lectin-bound smvECs are seen in the R2 gated population (data not shown).

Reverse-Transcription Polymerase Chain Reaction and Immunoblot Characterization of Endothelial Cell-Specific Molecules in Spinal Cord Microvascular Endothelial Cell Isolations

To determine the relative enrichment and purity of smvEC preparations at the mRNA and protein level, end-point reverse-transcription polymerase chain reaction (RT-PCR) and immunoblotting analyses were performed for EC and non-EC markers. Various mRNAs specifically expressed by smvECs were analyzed including PECAM-1, Glut-1, and claudin-5, all of which are specific to ECs in the adult mouse spinal cord (Figure 1). All of these mRNAs were amplified in samples of total RNA isolated from the spinal cord but were observed to be expressed at low levels relative to cyclophilin-A (Figures 3A and 3B). By contrast, these mRNAs were significantly enriched in total RNA isolated from smvECs (Figure 3B). This enrichment was further characterized using an EC-focused qRT-PCR microarray. In these experiments, the majority of mRNAs associated with ECs were highly enriched as compared with the total spinal cord (Supplementary Figure 4). Of all species analyzed, 15 selected mRNAs specifically expressed in the adult mouse spinal cord ECs (identified as class II mRNAs) showed an average 23-fold enrichment compared with amplification from total spinal cord RNA (Supplementary Figure 1). Furthermore, mRNAs known to be expressed in the EC compartment as well as in other cells of the adult spinal cord (identified as class I mRNAs) were approximately fourfold enriched compared with total spinal cord. Conversely, no amplification was observed for mRNAs associated with other NVU cellular compartments, including neurons (Map2), astrocytes (GFAP), and pericytes (Desmin) (Figures 3C and 3D and Supplementary Figure 2, respectively). The only exception was claudin-11 (OSP-1) (Figures 3C and 3D). This was quite unexpected because this marker is traditionally used to identify oligodendrocytes but this transcript has been detected in rat brain-derived ECs (Enerson and Drewes, 2006), suggesting that this result may be indicative not only of the significant presence of oligodendroglial mRNAs but also of an EC-expressed transcript unique to the CNS endothelium.

Using immunoblotting for both EC and non-EC-specific proteins, we have characterized the enrichment of the smvEC preparation at the protein level (Supplementary Figure 3). Western blotting for claudin-5 and occludin show a significant enrichment as compared with total spinal cord lysates, with claudin-5 protein levels more than 40-fold enriched in smvECs. Additionally, immunoblotting for GFAP, NSE, and 2′-3′-cyclic nucleotide 3′-phosphodiesterase (CNPase) show low, although detectable, levels of these non-EC proteins. These results show that the smvEC isolations allow for significant enrichment of EC-specific mRNAs and proteins but may be better suited for transcriptomic screening approaches based on immunoblotting characterization of the preparation.

Significant mRNA Dysregulation is Observed in Endothelial Cells Isolated from the Injured Spinal Cord

Of the approximately 90 genes of interest included on the qRT-PCR microarray plates, we were able to confidently resolve 60 in total RNA samples isolated from smvECs prepared from the acutely injured spinal cord (Supplementary Figure 5). Of these, 33 mRNAs were > 3-fold upregulated, 3 showed > 3-fold downregulation, and 18 mRNAs showed no dysregulation in ECs 24 h after SCI. The most dramatically upregulated EC mRNA was thrombospondin 1 (TSP-1), which was 58-fold upregulated (Figure 4). mRNA levels for chemokine ligand-5

(CCL5/RANTES) were 22-fold upregulated, and the secreted serine protease uPA was the third most highly upregulated mRNA (20-fold increase). By comparison, tissue plasminogen activator was not dysregulated in ECs after SCI. Conversely, the most highly down-regulated mRNA was that encoding McDonough feline sarcoma (FMS)-like tyrosine kinase 1 (Flt-1/VEGFR-1), which was decreased over sevenfold. Interestingly, mRNA levels for kinase insert domain protein receptor (Flk-1/VEGFR-2) were unchanged. These results illustrate a very specific cellular response to trauma, even within the same family of molecular effectors. Also noteworthy is the significant 3.8-fold downregulation of the EC tight junction component occludin, which is consistent with our previous results, indicating the loss of occludin immunoreactivity at the EC tight junction within days after SCI (Benton *et al*, 2008).

Immunohistochemical Validation of qRT-PCR Results Suggest Pathologically Relevant Overexpression of Thrombospondin 1 Protein in Affected Spinal Cord Microvascular Endothelial Cells

Thrombospondin 1 is one of the most potent negative regulators of both developmental and adaptive/pathologic angiogeneses in many tissues, including the CNS (Zhang and Lawler, 2007). To determine if the dramatic increases in TSP-1 mRNA are of any biologic consequence, immunohistochemical staining for TSP-1 was performed on the injured spinal cord tissue (Figure 5). In sham spinal cord tissue, little/no TSP-1 immuno-reactivity was observed in any cellular structure (Figure 5A). By 1 day after SCI, a marked increase in TSP-1 immunostaining was observed at the injury site and was associated with perfused microvascular profiles (Figure 5B, F). This EC-associated TSP-1 immunoreactivity was observed at 3 days after SCI (Figures 5C and 5G), but not at 7 days after SCI (data not shown). Apparent microvascular profiles in penumbral areas of the injury retain astroglial investment and exhibited TSP-1 immunostaining (Figure 5K). Colocalization of TSP-1 to the astroglial compartment is not observed (Figure 5L). Indeed, definitively identified microvascular profiles labeled by LEA perfusion and devoid of astroglial investment show significant TSP-1 immunoreactivity, with juxtaposed TSP-1 and LEA signal evident on close examination (Figure 5M and 5N). Colocalization of TSP-1 and PECAM-1 immuno-reactivity in vessels apparently devoid of perfusion (that is, FITC-LEA signal) suggests microvascular expression of TSP-1 in profiles lacking intravascular LEA signal (Figures 5O and 5P).

Increased Urokinase Plasminogen Activator Activity and Concomitant Plasminogen Activator System Component Induction after Spinal Cord Injury in Spinal Cord Microvascular Endothelial Cells

To determine if the significant induction of mRNA for uPA translates to enhanced proteolytic activity in the injured spinal cord, tissue was collected at 1 and 3 days after SCI and subjected to uPA zymography (Figure 6A). Quantitative analyses of these results (Figure 6B) show a significant increase in tissue levels of uPA activity 1 day after SCI, with tissue levels of uPA activity further increased 3 days after injury. Interestingly, a temporal correlation between uPA and plasmin activities (Figures 7M and 7N) was observed at 1 day after SCI, but tissue levels of plasmin activity were decreased by 3 days after injury, with a significant increase in tissue plasmin enzymatic activity observed 1 day after SCI. Immunohistochemical results showing increased microvascular levels of various members of the plasminogen activator system (PAS) suggest a role in pathologic activation at the NVU. For example, no appreciable immunostaining for the endogenous inhibitor of uPA, plasminogen activator inhibitor-1 (PAI-1), was observed in control spinal tissue (Figure 7A). By 3 days after SCI, significant PAI-1 immunoreactivity is observed in LEA-bound spinal microvessels (Figures 7C and 7D). Furthermore, an increase in uPA receptor (uPAR) immuno-reactivity was apparent at the same time point after SCI as compared with controls (Figures 7I and 7J). Interestingly, uPAR immunoreactivity is initially observed in sparse obstructed microvessels with intact astroglial investment (Figure 7K). This pattern of immunoreactivity is more widespread by 3 days after

SCI concomitant with re-perfusion and the loss of perivascular astrocytic investment (Figure 7L).

Discussion

Intravital Fluorescein Isothiocyanate-Lectin-Facilitated Isolation of Spinal Cord Microvascular Endothelial Cells

Previous studies have used various methodologies to characterize the basal transcriptome of CNS ECs (Shusta *et al*, 2002; Enerson and Drewes, 2006), but the current study is unique in several ways. First of all, combining existing methodologies, including intravital labeling of smvECs using FITC-lectin, we could obtain sufficient amounts of EC from small quantities of spinal tissue (≈100 mg) to generate transcriptomic data. In contrast, the aforementioned studies used several grams of CNS tissue as their biologic input. This enhanced sensitivity was facilitated by both the acute purity of the FACS-isolated smvECs and the qRT-PCR transcriptomic approach. Importantly, in spite of the differential methodologies used in our previous studies, consistent results were seen with respect to the multiple enriched EC mRNAs obtained. Of these, Glut-1 and claudin-5 are consistently enriched in preparations of human (Shusta *et al*, 2002) and rat (Enerson and Drewes, 2006) brain-derived ECs. The current methodology results in very rapid (≈1.5 h) isolation of high-purity ECs from the spinal cord. This is compared with variable lengths of time required for the more commonly applied gradient centrifugation isolation of CNS-derived ECs, with the more rapid isolation (≈1 h) associated with appreciable amounts of non-EC contribution to the preparation (Enerson and Drewes, 2006). Longer protocols (≈4 to 8 h) yield preparations of higher purity (Wu *et al*, 2003), but are not optimal for transcriptomic assessment of pathologic activation because of the potential for degradation of targets. Finally, the current study represents the initial report isolating traumatically injured smvECs to identify mRNAs dysregulated in pathologically activated ECs.

One potential shortcoming of the current isolation method developed relates to an apparent decrease in cellular viability after lectin-FACS isolation (data not shown). Although having no impact on the immediate use of the ECs obtained for various biochemical analyses, we have been unable to obtain viable long-term EC cultures, which is in contrast to previously described isolation methods (Wu *et al*, 2003; Ge and Pachter, 2006). It is likely that the current isolation method induces significant cellular stress, resulting in the observed diminished EC viability *in vitro*. Efforts are ongoing regarding further methodological optimization to facilitate their propagation in primary culture.

The Endothelial Cell Transcriptome is Acutely Dysregulated after Spinal Cord Injury

Several studies have shown that SCI results in profound and immediate loss of blood vessels at the injury epicenter followed by a pathologic angiogenesis in the affected tissue (Loy *et al*, 2002; Casella *et al*, 2002; Whetstone *et al*, 2003; Benton *et al*, 2008). However, little is known regarding the acute molecular events occurring in the ECs driving this vascular plasticity. The current results provide novel insight into the early transcriptional events preceding these established pathologic cascades by identifying candidate molecular pathway(s) responsible for the pathologic EC induction that may hold therapeutic promise. Recent studies in rats have shown profound induction of apoptosis (up to 80% of affected ECs) within 24 h of SCI as assessed by TUNEL (terminal deoxynucleotidyl transferase biotin-dUTP nick end labeling) staining and nuclear morphology (Casella *et al*, 2006), although specific regulators of this response were not identified. Consistent with this observation we show that many proapoptotic mRNAs are increased in the EC compartment 24 h after SCI, including caspase-3, caspase-6, Cflar, and RhoB, with the latter species being one of the most highly induced mRNAs observed (see Supplementary Figure 5). This response is relevant in the context of SCI as RhoB potently

affects EC survival during periods of vascular plasticity (Adini *et al*, 2003). Conversely, levels of various antiapoptotic mRNAs, including Bcl2l1, Birc1a, and Birc2, are unchanged in smvECs after SCI. Taken together, these results define multiple candidate apoptotic cascades induced in smvECs after SCI, complementing previous studies by providing evidence of specific mechanisms for established histopathology.

Also important is the finding that multiple mRNAs involved in neuroinflammation are induced in ECs after SCI. Of these, RANTES/CCL5 showed the most striking upregulation. mRNA levels for this potent chemokine increase in the injured mouse spinal cord, persisting for up to 21 days after SCI and is associated with the areas of T-cell activation and infiltration (Jones *et al*, 2005), although the cellular source of the chemokine is not elucidated. The finding that RANTES/CCL5 mRNA levels are dramatically increased 24 h after SCI in smvECs identifies a putative novel cellular source of this chemokine after contusive SCI. These data suggest a direct contribution of the injured microvascular endothelium to inflammatory chemokine cascades in the injured spinal cord. This implication is further supported by the finding that mRNAs for multiple mediators of inflammation are increased in ECs after SCI, including CXCR-5, GM-CSF, interferon-β1, interleukins-3, -6, and -11, as well as E- and P-selectin (Supplementary Figure 5).

Thrombospondin-1 and Adaptive Angiogenesis in Spinal Cord Injury

The most striking result in this study is the dramatic increase in EC TSP-1 mRNA 24 h after SCI and a correlative increase in protein expression. To date, no data exist regarding the role of TSP-1 in EC survival in the injured spinal cord. Thrombospondin 1 decreases angiogenesis by inhibiting EC proliferation by multiple mechanisms, including the induction of caspase-dependent apoptosis (Zhang and Lawler, 2007). Thus, in light of the results regarding the potentiation of several caspase isoforms, this cellular response to the TSP-1 production in the context of SCI is feasible, as overexpression and apparent autocrine stimulation of apoptosis in ECs by TSP-1 action in the injured CNS has been documented previously (Lin *et al*, 2003). In that study, TSP-1 activation of a CD36-Fyn-Caspase-3-p38 MAPK cascade was essential for TSP-1′s anti-angiogenic/proapoptotic effect, partly by increased expression of the Fas ligand (FasL) (Jimenez *et al*, 2000). Relevant to this, in this study, we show FasL to be elevated in the ECs (7.6-fold increase; $P = 0.0661$), further supporting the implication of TSP-1 in EC death after SCI.

Plasminogen Activator System Regulation of Vascular Function after Spinal Cord Injury

To date, several studies have implicated various components of the PAS in the EC activation and adaptive angiogenic responses in the CNS. For example, uPA and PAI-1 are upregulated in neovascular ECs of malignant brain tumors (Arai *et al*, 1998). Furthermore, PAI-1 (Zhang *et al*, 1999) and uPAR (Nagai *et al*, 2008) are all elevated in cortical mvECs after experimental stroke. Furthermore, the attenuation of uPA activity in experimental stroke reduces infarct volume (Hamann *et al*, 2004). Importantly, this response appears to be clinically relevant because these components are also found to be increased in human stroke foci (Dietzmann *et al*, 2000) and traumatic brain injury (Beschorner *et al*, 2000). The role of uPA in the injured spinal cord is wholly unknown, although very recently, uPA levels were shown to increase after SCI (Minor and Seeds, 2008). The results of this study are consistent with this finding and extend it by showing EC compartmentalization of this response.

Although the pathologic potential of increased uPA and/or plasmin activity is relatively clear, the initiation factor for increased PAS component expression in the EC compartment after SCI is at present speculative. One potential mechanism for the observed upregulation of uPA may be related to the action of TSP-1. Thrombospondin 1 increases uPA expression in metastatic tumors (Albo *et al*, 1999). Although this is an intriguing possibility in light of the robust

upregulation of TSP-1 in this study, the connection between these two molecular events in ECs after SCI awaits elucidation. Another possible candidate for this induction is the potent vasoactive molecule VEGF (vascular endothelial growth factor), because it is known to induce uPA expression in activated endothelium (Prager *et al*, 2004). This connection is plausible as VEGF levels are rapidly and dramatically increased in the injured spinal cord (Skold *et al*, 2000). In addition, similar to TSP-1, TGF-β1 (transforming growth factor-β1) signaling results in increased expression of both uPA and PAI-1, the latter of which is also significantly increased in smvECs after SCI (Supplementary Figure 5). Interestingly, a reciprocal relationship exists between uPA/plasmin activation and TGF-β1, because liberation of latent TGF-β1 isoforms from the extracellular matrix is PAS-dependent both *in vivo* and *in vitro* (Rifkin *et al*, 1999). Considering the potential for this feed-forward loop of bioactivity, as well as a possible role in the induction of TSP-1 expression in the EC compartment, current efforts are focused on further examination of a role for TGF-β1 pathologic NVU plasticity and dysfunction after SCI.

Supplementary Material

Refer to Web version on PubMed Central for supplementary material.

Acknowledgements

We thank Mrs Christine Nunn and Mrs Kim Fentress for valuable experimental surgical support and perioperative care of experimental animals and thank Ms Darlene Burke for assistance with statistical analyses. We also thank Dr David SK Magnuson for critical comments and feedback related to various aspects of methodologic development.

This research was supported by NS045734, RR15576, Norton Healthcare, and by the Commonwealth of Kentucky Challenge for Excellence (SRW and TH).

References

Adini I, Rabinovitz I, Sun JF, Prendergast GC, Benjamin LE. RhoB controls Akt trafficking and stage-specific survival of endothelial cells during vascular development. Genes Dev 2003;17:2721–32. [PubMed: 14597666]

Albo D, Berger DH, Rothman VL, Tuszynski GP. Role of urokinase plasminogen activator receptor in thrombospondin 1-mediated tumor cell invasion. J Surg Res 1999;82:331–8. [PubMed: 10090848]

Arai Y, Kubota T, Nakagawa T, Kabuto M, Sato K, Kobayashi H. Production of urokinase-type plasminogen activator (u-PA) and plasminogen activator inhibitor-1 (PAI-1) in human brain tumours. Acta Neurochir (Wien) 1998;140:377–85. [PubMed: 9689330]

Benton RL, Maddie MA, Minnillo DR, Hagg T, Whittemore SR. Griffonia simplicifolia isolectin B4 identifies a specific subpopulation of angiogenic blood vessels following contusive spinal cord injury in the adult mouse. J Comp Neurol 2008;507:1031–52. [PubMed: 18092342]

Beschorner R, Schluesener HJ, Nguyen TD, Magdolen V, Luther T, Pedal I, Mattern R, Meyermann R, Schwab JM. Lesion-associated accumulation of uPAR/. Neuropathol Appl Neurobiol 2000;26:522–7. [PubMed: 11123718]

Bullock R, Fujisawa H. The role of glutamate antagonists for the treatment of CNS injury. J Neurotrauma 1992;9(Suppl 2):S443–62. [PubMed: 1613806]

Casella GT, Bunge MB, Wood PM. Endothelial cell loss is not a major cause of neuronal and glial cell death following contusion injury of the spinal cord. Exp Neurol 2006;202:8–20. [PubMed: 16872600]

Casella GT, Marcillo A, Bunge MB, Wood PM. New vascular tissue rapidly replaces neural parenchyma and vessels destroyed by a contusion injury to the rat spinal cord. Exp Neurol 2002;173:63–76. [PubMed: 11771939]

Dietzmann K, von BP, Krause D, Wittig H, Mawrin C, Kirches E. Expression of the plasminogen activator system and the inhibitors PAI-1 and PAI-2 in posttraumatic lesions of the CNS and brain injuries following dramatic circulatory arrests: an immunohistochemical study. Pathol Res Pract 2000;196:15–21. [PubMed: 10674268]

Diglio CA, Grammas P, Giacomelli F, Wiener J. Primary culture of rat cerebral microvascular endothelial cells. Isolation, growth, and characterization. Lab Invest 1982;46:554–63. [PubMed: 7045518]

Ducker TB, Assenmacher DR. Microvascular response to experimental spinal cord trauma. Surg Forum 1969;20:428–30. [PubMed: 4986409]

Enerson BE, Drewes LR. The rat blood—brain barrier transcriptome. J Cereb Blood Flow Metab 2006;26:959–73. [PubMed: 16306934]

Ge S, Pachter JS. Isolation and culture of micro-vascular endothelial cells from murine spinal cord. J Neuroimmunol 2006;177:209–14. [PubMed: 16806499]

Geisler FH, Coleman WP, Grieco G, Poonian D. The Sygen multicenter acute spinal cord injury study. Spine 2001;26:S87–98. [PubMed: 11805614]

Grasso G, Sfacteria A, Erbayraktar S, Passalacqua M, Meli F, Gokmen N, Yilmaz O, La TD, Buemi M, Iacopino DG, Coleman T, Cerami A, Brines M, Tomasello F. Amelioration of spinal cord compressive injury by pharmacological preconditioning with erythropoietin and a nonerythropoietic erythropoietin derivative. J Neurosurg Spine 2006;4:310–8. [PubMed: 16619678]

Hamann GF, Burggraf D, Martens HK, Liebetrau M, Jager G, Wunderlich N, DeGeorgia M, Krieger DW. Mild to moderate hypothermia prevents micro-vascular basal lamina antigen loss in experimental focal cerebral ischemia. Stroke 2004;35:764–9. [PubMed: 14976330]

Hemmings SJ, Storey KB. Brain gamma-glutamyl-transpeptidase: characteristics, development and thyroid hormone dependency of the enzyme in isolated microvessels and neuronal/glial cell plasma membranes. Mol Cell Biochem 1999;202:119–30. [PubMed: 10706002]

Jimenez B, Volpert OV, Crawford SE, Febbraio M, Silverstein RL, Bouck N. Signals leading to apoptosis-dependent inhibition of neovascularization by thrombospondin-1. Nat Med 2000;6:41–8. [PubMed: 10613822]

Jones TB, Hart RP, Popovich PG. Molecular control of physiological and pathological T-cell recruitment after mouse spinal cord injury. J Neurosci 2005;25:6576–83. [PubMed: 16014718]

Joo F, Dux E, Szucs A. Microvessels from the spinal cord: isolation procedure and characterization of the fraction. J Neurochem 1982;39:263–6. [PubMed: 6123551]

Lin T, Kim G-M, Chen J-J, Cheung W-M, He Y, Hsu C. Differential regulation of thrombospondin-1 and thrombospondin-2 after focal cerebral ischemia/reperfusion. Stroke 2003;34:177–86. [PubMed: 12511771]

Lin Y, Vreman HJ, Wong RJ, Tjoa T, Yamauchi T, Noble-Haeusslein LJ. Heme oxygenase-1 stabilizes the blood—spinal cord barrier and limits oxidative stress and white matter damage in the acutely injured murine spinal cord. J Cereb Blood Flow Metab 2007;27:1010–21. [PubMed: 17047682]

Loy DN, Crawford CH, Darnall JB, Burke DA, Onifer SM, Whittemore SR. Temporal progression of angio-genesis and basal lamina deposition after contusive spinal cord injury in the adult rat. J Comp Neurol 2002;445:308–24. [PubMed: 11920709]

Means ED, Anderson DK. Neuronophagia by leukocytes in experimental spinal cord injury. J Neuropathol Exp Neurol 1983;42:707–19. [PubMed: 6631457]

Minor KH, Seeds NW. Plasminogen activator induction facilitates recovery of respiratory function following spinal cord injury. Mol Cell Neurosci 2008;37:143–152. [PubMed: 18042398]

Nagai N, Okada K, Kawao N, Ishida C, Ueshima S, Collen D, Matsuo O. Urokinase-type plasminogen activator receptor (uPAR) augments brain damage in a murine model of ischemic stroke. Neurosci Lett 2008;432:46–49. [PubMed: 18164548]

Noble LJ, Wrathall JR. Correlative analyses of lesion development and functional status after graded spinal cord contusive injuries in the rat. Exp Neurol 1989;103:34–40. [PubMed: 2912748]

Pannu R, Christie DK, Barbosa E, Singh I, Singh AK. Post-trauma Lipitor treatment prevents endothelial dysfunction, facilitates neuroprotection, and promotes locomotor recovery following spinal cord injury. J Neurochem 2007;101:182–200. [PubMed: 17217414]

Prager GW, Breuss JM, Steurer S, Olcaydu D, Mihaly J, Brunner PM, Stockinger H, Binder BR. Vascular endothelial growth factor receptor-2-induced initial endothelial cell migration depends on the presence of the urokinase receptor. Circ Res 2004;94:1562–70. [PubMed: 15131009]

Rifkin DB, Mazzieri R, Munger JS, Noguera I, Sung J. Proteolytic control of growth factor availability. APMIS 1999;107:80–5. [PubMed: 10190283]

Shusta EV, Boado RJ, Mathern GW, Pardridge WM. Vascular genomics of the human brain. J Cereb Blood Flow Metab 2002;22:245–52. [PubMed: 11891429]

Skold M, Cullheim S, Hammarberg H, Piehl F, Suneson A, Lake S, Sjogren A, Walum E, Risling M. Induction of VEGF and VEGF receptors in the spinal cord after mechanical spinal injury and prostaglandin administration. Eur J Neurosci 2000;12:3675–86. [PubMed: 11029637]

Whetstone WD, Hsu JY, Eisenberg M, Werb Z, Noble-Haeusslein LJ. Blood—spinal cord barrier after spinal cord injury: relation to revascularization and wound healing. J Neurosci Res 2003;74:227–39. [PubMed: 14515352]

Wu Z, Hofman FM, Zlokovic BV. A simple method for isolation and characterization of mouse brain microvascular endothelial cells. J Neurosci Methods 2003;130:53–63. [PubMed: 14583404]

Yang GY, Betz AL, Chenevert TL, Brunberg JA, Hoff JT. Experimental intracerebral hemorrhage: relationship between brain edema, blood flow, and blood—brain barrier permeability in rats. J Neurosurg 1994;81:93–102. [PubMed: 8207532]

Yousif S, Marie-Claire C, Roux F, Scherrmann JM, Decleves X. Expression of drug transporters at the blood—brain barrier using an optimized isolated rat brain microvessel strategy. Brain Res 2007;1134:1–11. [PubMed: 17196184]

Zhang X, Lawler J. Thrombospondin-based anti-angiogenic therapy. Microvasc Res 2007;74:90–9. [PubMed: 17559888]

Zhang ZG, Chopp M, Goussev A, Lu D, Morris D, Tsang W, Powers C, Ho KL. Cerebral microvascular obstruction by fibrin is associated with upregulation of PAI-1 acutely after onset of focal embolic ischemia in rats. J Neurosci 1999;19:10898–907. [PubMed: 10594071]

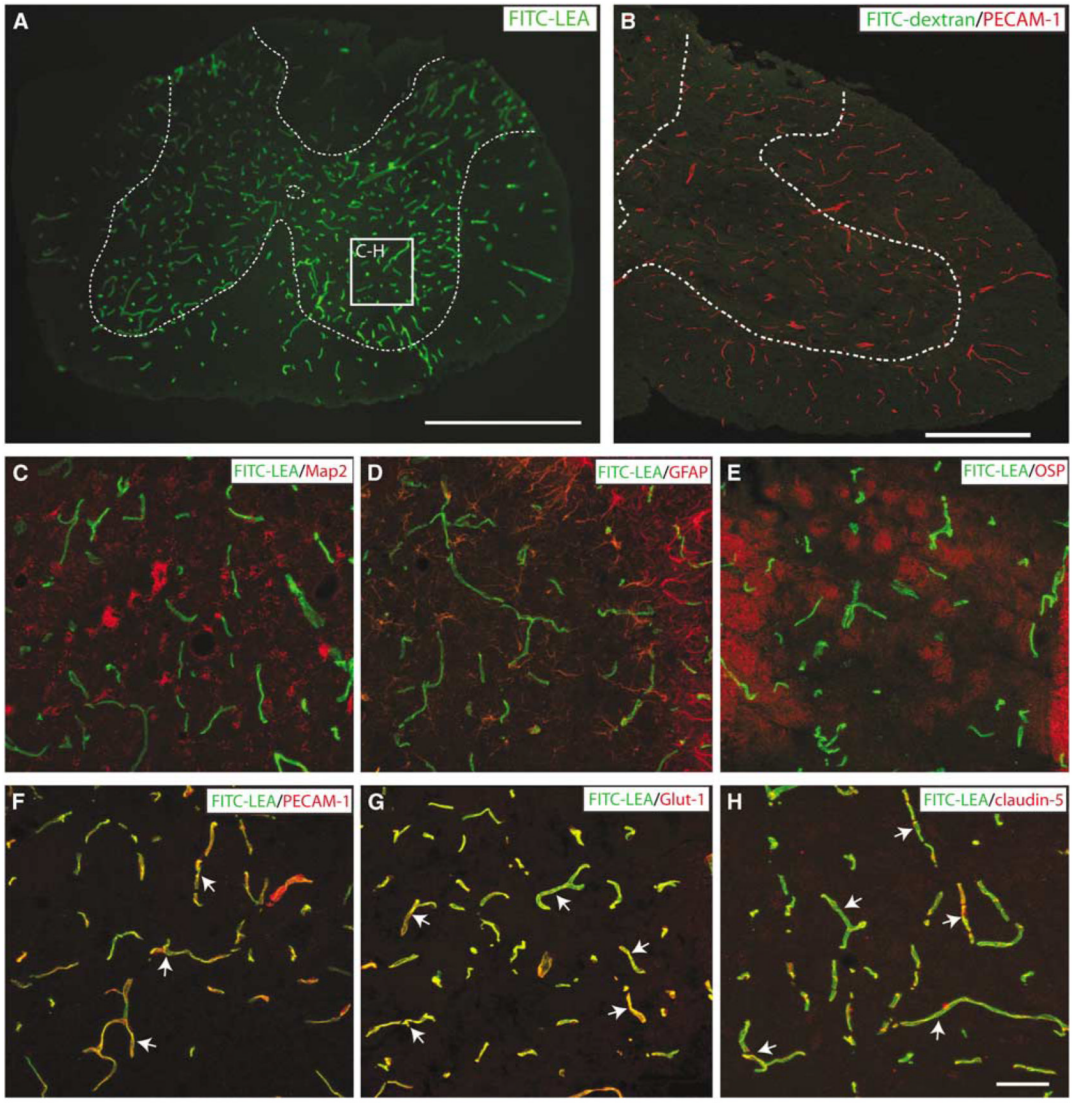

Figure 1.

Intravascular administration of FITC-LEA specifically binds glycoconjugates associated with the luminal glycocalyx of all perfused spinal microvessels in the normal adult mouse spinal cord. The relative hypervascularity of spinal gray matter is apparent (**A**; gray matter is outlined with dashed line). The specific interaction of FITC-LEA with spinal ECs is apparent in high-magnification insets (**C** to **H**). No colocalization of FITC-LEA is observed with neuronal elements (**C**), astrocytes (**D**), or oligodendrocytes (**E**) as shown by immunoreactivity for Map2, GFAP, or OSP, respectively. Conversely, double labeling of FITC-LEA with the vascular EC markers PECAM-1 (**F**; arrows), Glut-1 (**G**; arrows), and claudin-5 (**H**; arrows) is apparent. The specificity of the interaction between FITC-LEA and the glycocalyx of spinal vascular ECs is further shown by a lack of microvascular labeling when a molecular-weight-matched FITC-dextran is administered intravascularly (**B**; gray/white matter boundary indicated by the dashed line). Scale bars = 500 μm (**A**); 250 μm (**B**); 50 μm (**C** to **H**).

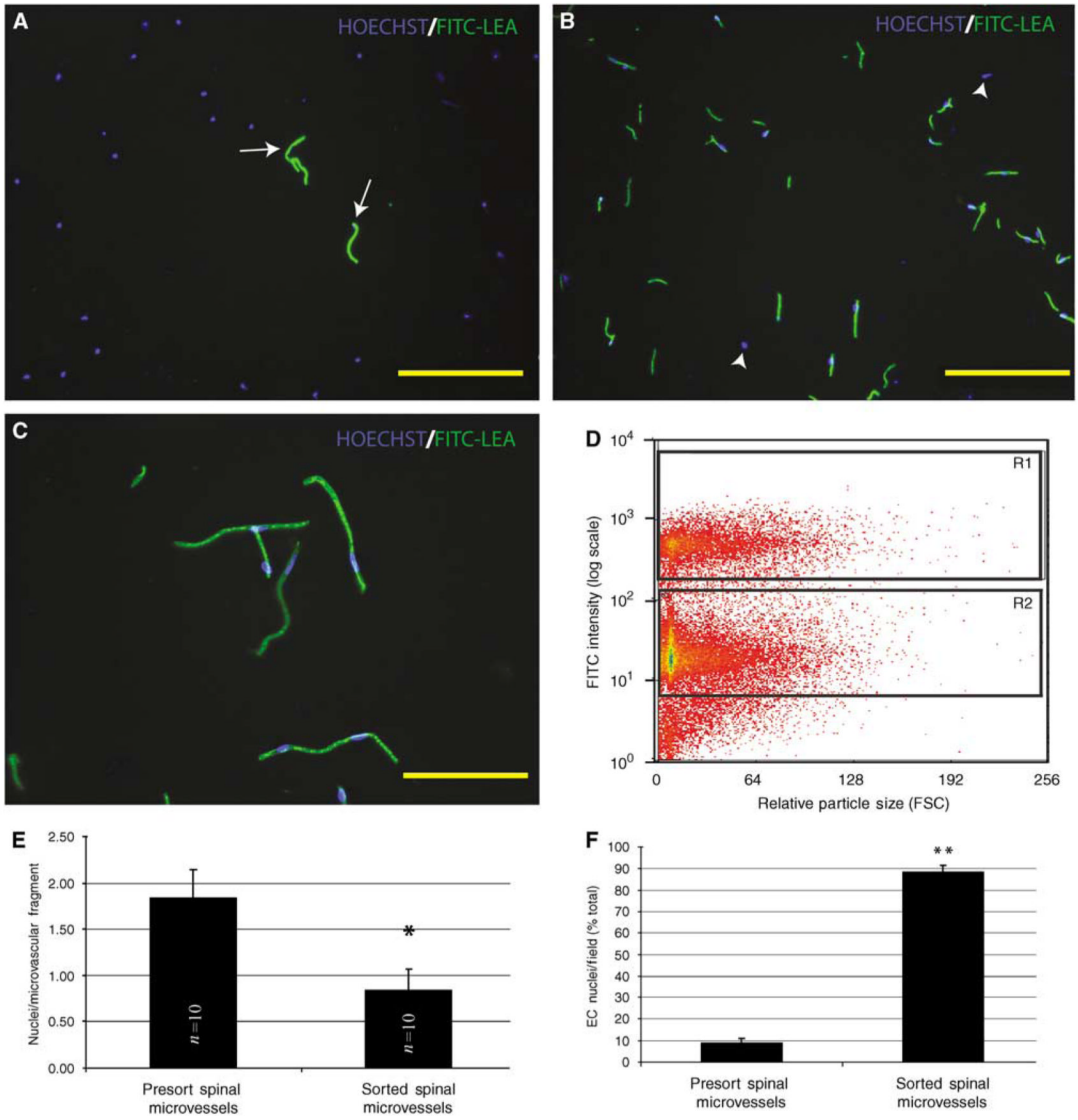

Figure 2.

Fluorescence-activated cell sorter isolation of FITC-LEA-infused spinal microvascular fragments results in a highly enriched population of smvECs. In presort spinal cord homogenates prepared from spinal tissue of FITC-LEA-infused mice, Hoechst-labeled EC nuclei account for a minority of cellular profiles (**A**; arrows). After FACS isolation of FITC-LEA-bound smvECs, few nuclei are present that are not intimately associated with microvascular fragments (**B**; arrowheads). Immediately after isolation, the microvascular fragments maintain their characteristic morphologic features with very few nonassociated nuclei apparent (**C**). A representative FACS plot (**D**) shows the labeled smvECs showing fluorescence approximately one order of magnitude greater than the background associated with the sample and clearly separating into the selected gate (R1) that contains the smvEC isolation. Quantitative analysis indicates that isolated smvECs have significantly fewer nuclei per FITC-LEA-bound microvascular fragment of the average nuclei per fragment (**E**) illustrates that smvECs experience significant shear stress as they are collected. Microscopic analyses of FACS-isolated smvEC collections show that approximately 90% of nuclei are associated with FITC-LEA microvascular fragments, a significant increase compared with total presort spinal

homogenates. Quantitative assessment of microvascular fragment isolation is expressed as mean±s.d. (n = 10 per experimental group) *sorted is significantly different from presort (d.f. = 16; $P = 4.04 \times 10^{-7}$) and **sorted is significantly different from presort (d.f. = 14; $P = 1.32 \times 10^{-18}$). Scale bars = 150 μm (**A**, **B**); 50 μm (**C**).

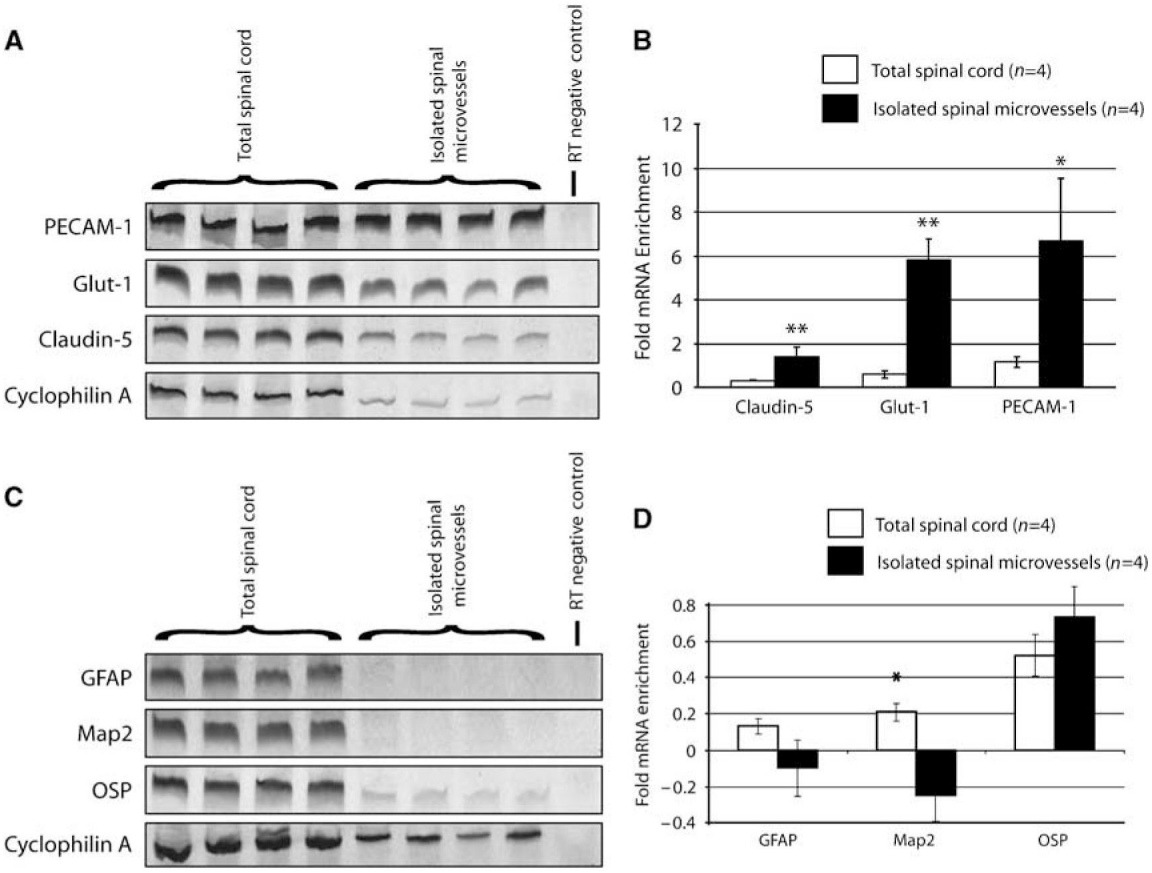

Figure 3.

Significant enrichment of EC mRNAs is observed in the smvEC preparation as compared with total spinal cord RNA samples. Several EC-specific mRNAs were examined by RT-PCR of RNA isolated from control spinal tissue or smvECs isolated from the intact adult mouse spinal cord (**A**). Quantitative analysis of results (**B**) show a relative enrichment for claudin-5 (1.39-fold; $P < 0.01$), Glut-1 (5.85-fold; $P < 0.01$), and PECAM-1 (6-7-fold; $P < 0.05$). By contrast, no significant enrichment of mRNAs expressed by astrocytes (GFAP), neurons (Map2), or oligodendrocytes (OSP) was observed in smvEC preparations as compared with total spinal cord samples (**C** and **D**). All quantitative data are expressed as the mean±s.d. ($n = 4$ per experimental group). *$P < 0.05$, **$P < 0.01$.

Upregulated mRNAs

RefSeq	Description	Gene name	Fold dysregulation	*P*-value
NM_011580	Thrombospondin 1	TSP-1/TSP1	58.12	0.0003
NM_013653	*Chemokine (C-C motif) ligand 5*	*CCL5/RANTES*	*22.05*	*0.004*
NM_008873	Plasminogen activator, urokinase	u-PA/uPA	20.52	0.003
NM_007483	Ras homolog gene family, member B	RhoB/Arh6	16.88	0.016
NM_008726	*Natriuretic peptide precursor type B*	*AA408272/BNP*	*15.83*	*0.0003*

Nondysregulated mRNAs

RefSeq	Description	Gene name	Fold dysregulation	*P*-value
NM_009673	Annexin A5	Anx5	1.14	0.580
NM_007527	*Bcl2-associated X protein*	*BAX*	*1.17*	*0.746*
NM_009743	Bcl2-like 1	Bcl(X)L/Bcl-XL	−1.24	0.338
NM_007465	*Baculoviral IAP repeat-containing 2*	*cIAP2/Api1*	*1.61*	*0.396*
NM_009142	Chemokine (C-X3-C motif) ligand 1	Cxc3/Scyd1	1.32	0.543
NM_007987	*Fas (TNF receptor superfamily member)*	*CD95/APO-1*	*1.51*	*0.507*
NM_010233	Fibronectin 1	Fn-1	1.66	0.100
NM_010612	Kinase insert domain protein receptor	VEGFR-2/Flk-1	−1.99	0.351
NM_008872	Plasminogen activator, tissue	tPA	−1.13	0.808
NM_009505	Vascular endothelial growth factor A	VEGF-A/VEGF120	1.03	0.946

Downregulated mRNAs

RefSeq	Description	Gene name	Fold dysregulation	*P*-value
NM_010228	FMS-like tyrosine kinase 1	VEGFR-1/Flt-1	−7.78	0.001
NM_007428	Occludin	Ocln	−3.79	0.011
NM_008756	Angiotensinogen (serpin peptidase inhib-8)	Al265500/Aogen	−3.40	0.033

Figure 4.

Focused qRT-PCR-based microarray analysis shows altered mRNA expression is observed in the smvECs 24 h after SCI. Presented are the top five upregulated, select nondysregulated, and all downregulated transcripts analyzed. Italicized results represent $n = 3$ and all other results are represented by $n = 4$.

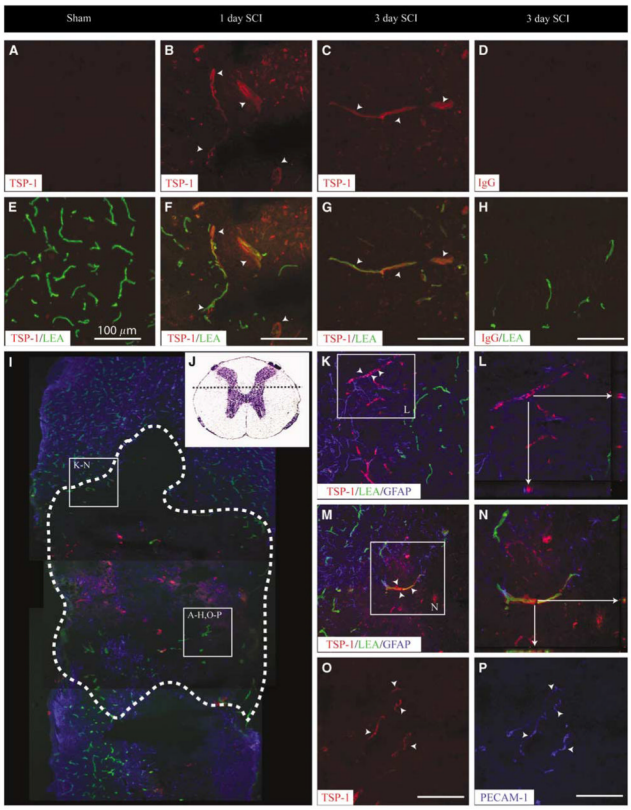

Figure 5.

Thrombospondin 1 protein levels are acutely increased in ECs after SCI. In the uninjured spinal cord, no TSP-1 expression is observed in perfused microvascular profiles (**A**, **E**). By 1 day after SCI, TSP-1 immunoreactivity is observed and is associated with spinal microvessels (**B**, **F**). This vascular expression pattern is maintained through 3 days after injury (**C**, **G**). Laser confocal microscopic examination of the immunoreactive signal for TSP-1 in spinal microvessels 24 h after SCI shows an EC localization, which is apparent in microvessels with and intact astroglial investment (**K**, **L**) as well those found in the epicenter tissue devoid of astrocytes (**M**, **N**). Interestingly, TSP-1 expression is observed in microvascular elements lacking binding of the perfusion marker (**L**, arrowheads) but is shown to be vascular profiles as determined by the colocalization of TSP-1 with the microvascular EC marker PECAM-1 in LEA-negative profiles (**O**, **P**; arrowheads). Thrombospondin 1-immunopositive microvessels are observed at both the injury epicenters (**A** to **H**, **O** to **P**) as well as in penumbral zones (**K** to **N**). A representative photomicrograph of the longitudinal view of the lesion at 24 h after SCI (**I**, dashed outline) illustrated the relative hypovascularity at the contusion site as compared with the spared spinal parenchyma. The spinal cord area represented in high-magnification photomicrographs is illustrated by the histologic preparation (**J**, dashed line). All scale bars = 100 μm.

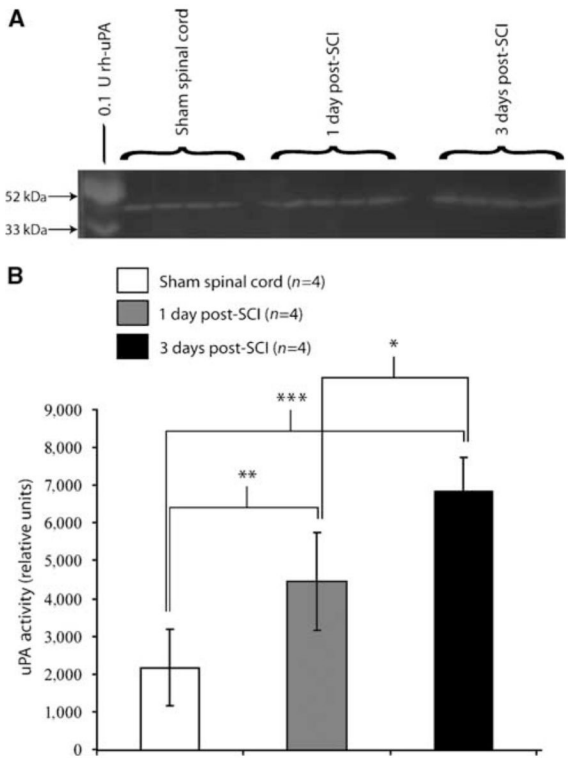

Figure 6.

Urokinase plasminogen activator enzymatic activity is increased in the contused mouse spinal cord. Urokinase plasminogen activator zymographic results (**A**) show detectable uPA enzyme activity in control spinal tissue. After SCI, tissue levels of uPA enzyme activity are markedly increased by 1 and 3 days after injury. (**B**) Quantitative analysis of zymographic results show uPA levels significantly elevated at 1 day after SCI as compared with controls, with spinal levels further elevated at 3 days after injury (*$P < 0.05$, **$P < 0.01$, ***$P < 0.001$; $F = 18.7$, d.f. = 2, 9). Quantitative data are expressed as mean±s.d.

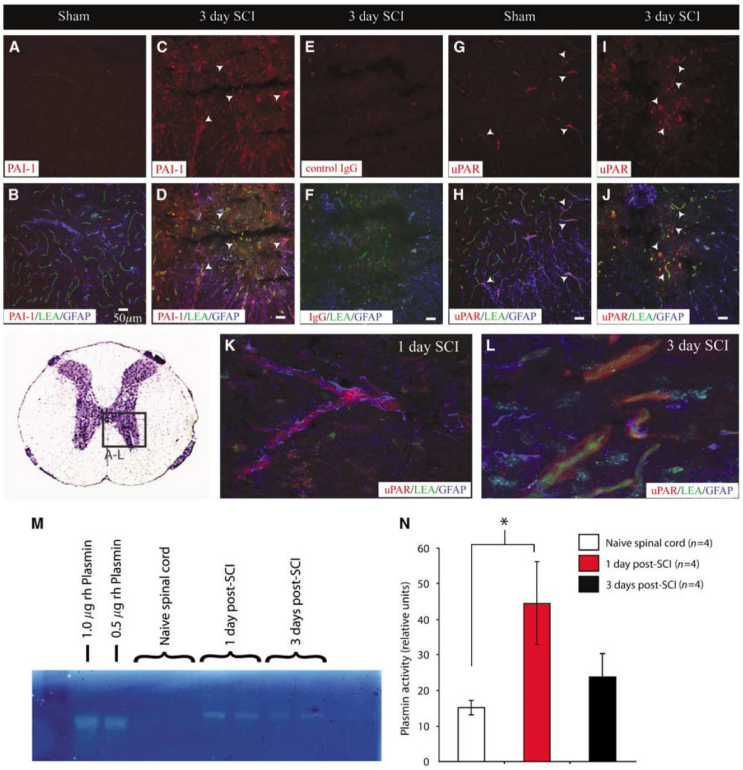

Figure 7.

Plasminogen activator system components are pathologically expressed by smvECs after SCI. Results from immunohistochemical validation of microarray results show a dramatic increase in PAI-1 levels in spinal microvessels 3 days after SCI (**C**, **D**), with very little immunostaining observed in control spinal tissue (**A**, **B**). The increase of uPA within ECs is of biological consequence as uPA receptor (uPAR) is present concomitant with this increase in uPA at the NVU (**K** to **N**). Interestingly, uPAR expression is observed in ECs 1 day after SCI with preserved astroglial investment (**K**), with levels of expression remaining high for up to 3 days after injury correlated with astroglial loss from the NVU (**L**). Zymographic analysis of plasmin enzyme activity in spinal tissue after SCI shows a temporal course of elevation consistent with that for uPA (**M**, **N**) showing the pathologic importance of the PAS induction for activation of this potent serine protease. Scale bars = 50 μm. Quantitative data are represented as the mean ±s.d. (*$P < 0.05$).